The Canadian Mineralogist
Vol. 45, pp. 1229-1245 (2007)
DOI: 10.2113/gscanmin.45.5.1229

PIZGRISCHITE, (Cu,Fe)$Cu_{14}PbBi_{17}S_{35}$, A NEW SULFOSALT FROM THE SWISS ALPS: DESCRIPTION, CRYSTAL STRUCTURE AND OCCURRENCE

NICOLAS MEISSER[§]

Musée Cantonal de Géologie and Institut de Minéralogie et Géochimie, Université-Dorigny, CH–1015 Lausanne, Switzerland

KURT SCHENK

Laboratoire de Cristallographie 1, EPFL, Dorigny, CH–1015 Lausanne, Switzerland

PETER BERLEPSCH

Heinrichsgasse 8, CH–4055 Basel, Switzerland

JOËL BRUGGER

School of Earth and Environmental Sciences, The University of Adelaide, North Terrace, 5005 Adelaide, South Australia, and Division of Mineralogy, South Australian Museum, North Terrace, 5000 Adelaide, South Australia

MICHEL BONIN

Laboratoire de Cristallographie 1, EPFL, Dorigny, CH–1015 Lausanne, Switzerland

ALAN J. CRIDDLE[†]

Department of Mineralogy, Natural History Museum, Cromwell Road, London SW7 580, U.K,

PHILIPPE THÉLIN AND FRANÇOIS BUSSY

Institut de Minéralogie et Géochimie, Université-Dorigny, CH–1015 Lausanne, Switzerland

ABSTRACT

Pizgrischite, (Cu,Fe)$Cu_{14}PbBi_{17}S_{35}$, is a new mineral species named after the type locality, Piz Grisch Mountain, Val Ferrera, Graubünden, Switzerland. This sulfosalt occurs as thin, striated, metallic lead-grey blades measuring up to 1 cm in length, embedded in quartz and associated with tetrahedrite, chalcopyrite, pyrite, sphalerite, emplectite and derivatives of the aikinite–bismuthinite series. In plane-polarized light, the new species is brownish grey with no perceptible pleochroism; under crossed nicols in oil immersion, it presents a weak anisotropy with dark brown tints. Minimum and maximum reflectance values (in %) in air are: 40.7–42.15 (470 nm), 41.2–43.1 (546 nm), 41.2–43.35 (589 nm) and 40.7–43.3 (650 nm). Cleavage is perfect along {001} and well developed on {010}. Abundant polysynthetic twinning is observed on (010). The mean micro-indentation hardness is 190 kg/mm^2 (Mohs hardness 3.3), and the calculated density is 6.58 g/cm^3. Electron-microprobe analyses yield (wt%; mean result of seven analyses): Cu 16.48, Pb 2.10, Fe 0.77, Bi 60.70, Sb 0.35, S 19.16, Se 0.04, total 99.60. The resulting empirical chemical formula is $(Cu_{15.24}Fe_{0.80}Pb_{0.60})_{\Sigma 16.64}(Bi_{17.07}Sb_{0.17})_{\Sigma 17.24}(S_{35.09}Se_{0.03})_{\Sigma 35.12}$, in accordance with the formula derived from the single-crystal refinement of the structure, (Cu,Fe)$Cu_{14}PbBi_{17}S_{35}$. Pizgrischite is monoclinic, space group $C2/m$, with the following unit-cell parameters: a 35.054(2), b 3.91123(1), c 43.192(2) Å, β 96.713(4)°, V 5881.24 Å^3, $Z = 4$. The strongest seven X-ray powder-diffraction lines [d in Å (I)(hkl)] are: 5.364(40)($\bar{6}04$), 4.080(50)($\bar{8}05$), 3.120(40)(118), 3.104(68)($\bar{3}18$), 2.759(53)($\bar{9}11$), 2.752(44)(910) and 1.956(100)(020). The crystal structure is an expanded monoclinic derivative of kupčikite. Pizgrischite belongs to the cuprobismutite series of bismuth sulfosalts but, *sensu stricto*, it is not a homologue of cuprobismutite. At the type

§ *E-mail address*: nicolas.meisser@unil.ch
† Deceased 2nd May 2002.

locality, pizgrischite is the result of the Alpine metamorphism under greenschist-facies conditions of pre-Tertiary hydrothermal Cu–Bi mineralization.

Keywords: pizgrischite, new mineral species, sulfosalt, crystal structure, kupčikite, Alps, Switzerland.

Sommaire

La pizgrischite, (Cu,Fe)$Cu_{14}PbBi_{17}S_{35}$, est une nouvelle espèce minérale nommée d'après son lieu de découverte dans les Alpes, le Piz Grisch, montagne située dans le Val Ferrera, canton des Grisons, Suisse. Ce sulfosel se présente en fines lames striées à l'éclat métallique gris acier et qui mesurent jusqu'à 1 cm. Ces cristaux sont inclus dans du quartz et associés à la tétraédrite, la chalcopyrite, la pyrite, la sphalérite, l'emplectite et à des sulfosels de la série aïkinite–bismuthinite. Optiquement, en lumière simplement polarisée, le nouveau minéral est brun grisâtre sans pléochroïsme visible. Sous immersion dans l'huile et en lumière doublement polarisée, il présente une faible anisotropie optique avec des teintes brun foncé. Le clivage est excellent selon {001} et bien marqué selon {010}. Les valeurs minimales et maximales du pouvoir réflecteur dans l'air, en fonction de la longueur d'onde incidente, sont (en %): 40.7–42.15 (470 nm), 41.2–43.1 (546 nm), 41.2–43.35 (589 nm) et 40.7–43.3 (650 nm). Un abondant maclage polysynthétique s'observe dans le plan (010). La dureté par micro-indentation est de 190 kg/mm^2 (ce qui correspond à une dureté selon Mohs de 3.3), et la densité calculée, de 6.58. L'analyse chimique par microsonde électronique donne (en % poids; résultat moyen de sept analyses): Cu 16.48, Pb 2.10, Fe 0.77, Bi 60.70, Sb 0.35, S 19.16, Se 0.04, total 99.60. La formule chimique empirique est: $(Cu_{15.24}Fe_{0.80}Pb_{0.60})_{\Sigma 16.64}(Bi_{17.07}Sb_{0.17})_{\Sigma 17.24}(S_{35.09}Se_{0.03})_{\Sigma 35.12}$ et qui correspond bien avec celle obtenue par résolution de la structure cristalline: (Cu,Fe)$Cu_{14}PbBi_{17}S_{35}$. La pizgrischite est un sulfosel monoclinique, de groupe spatial *C*2/*m*, qui présente les paramètres réticulaires suivants: *a* 35.054(2), *b* 3.91123(1), *c* 43.192(2) Å, β 96.713(4)°, *V* 5881.24 Å^3, *Z* = 4. Les sept raies les plus intenses du cliché de diffraction par la méthode des poudres sont [*d* en Å (*I*)(*hkl*)]: 5.364(40)($\bar{6}$04), 4.080(50)($\bar{8}$05), 3.120(40)(118), 3.104(68)($\bar{3}$18), 2.759(53)($\bar{9}$11), 2.752(44)(910) et 1.956(100)(020). La structure cristalline est plus fortement expansée que celle de la kupčikite. La pizgrischite appartient à la série des sulfosels bismuthifères apparentés à la cuprobismutite; toutefois, il ne s'agit pas au sens strict d'un homologue de la cuprobismutite. Dans sa localité-type, la pizgrischite résulte du métamorphisme régional, en faciès schistes vert, d'un produit de minéralisation hydrothermale à cuivre et bismuth d'âge pré-Tertiaire.

Mots-clés: pizgrischite, nouvelle espèce minérale, sulfosel, structure cristalline, kupčikite, Alps, Suisse.

Introduction

The sulfosalt pizgrischite, (Cu,Fe)$Cu_{14}PbBi_{17}S_{35}$, is a new mineral species from an Alpine metamorphosed pre-Tertiary Cu–Bi quartz vein situated in the steep northern face of Piz Grisch, Val Ferrera, Graubünden, eastern Swiss Alps. Small stratabound Mn-deposits (*e.g.,* Fianel and Starlera) located in Triassic carbonates on the northwestern and southwestern face of Piz Grisch, are well known because of the occurrence of new or rare mineral species, in some cases in striking samples, described during the last decade (*i.e.,* fianelite, manganlotharmeyerite, ansermetite, sailaufite, wallkilldellite, romeite, tilasite, medaite, palenzonaite, and långbanite; Brugger & Berlepsch 1996, Brugger & Gieré 1999, 2000, Brugger *et al*. 2003a, b, Meisser *et al*. 2004).

The occurrence of an acicular sulfosalt at Piz Grisch was mentioned already by Grünenfelder (1956), who identified it as "wittichenite" on the basis of its optical properties. A new sampling was made in July 1988, and subsequent XRD analysis showed that the "wittichenite" is indeed an unknown mineral species.

The new mineral is named after the type locality, Piz Grisch mountain. The mineral was approved by the IMA Commission on New Minerals and Mineral Names (vote no. 2001–002). Two holotype specimens are deposited at the Museum of Geology, Lausanne (MGL), Switzerland: sample MGL 58622 consists of crystals isolated by dilute hydrofluoric acid and used for the single-crystal study, chemical analysis and synchrotron X-ray powder diffraction. Sample MGL 53660 is a polished section used for the measurement of optical data, for chemical analysis and a study of its paragenesis. A cotype sample is deposited at the British Museum of Natural History, London (BM–NH). All three specimens are fragments of a single hand-sized specimen.

Occurrence and Geological Setting

Occurrence

The Cu–Bi quartz vein containing pizgrischite is located in the face under the ridge extending to the northwest of Piz Grisch (3062 m), Val Ferrera, Graubünden, eastern Swiss Alps. The coordinates of the type locality according to the Swiss federal system are: 755.400/155.700; 2950 m. The access to this mineral occurrence is made difficult by its location in a cliff face, and climbing is necessary.

Mineral association

Sprays of pizgrischite crystals are embedded in fine-grained saccharoidal quartz. Other associated sulfides and sulfosalts form mm-sized masses dispersed in

quartz. Xenomorphic Bi-bearing tetrahedrite, $Cu_{11.07}Ag_{0.01}Fe_{1.29}Zn_{0.08}Sb_{2.88}As_{0.64}Bi_{0.48}S_{12.54}$ with 6.10 wt.% Bi (two analyses) is commonly partially replaced by flame-like inclusions of emplectite, $Cu_{0.99}Fe_{0.03}Bi_{0.97}Sb_{0.01}S_{2.00}Se_{0.01}$ (four analyses) and idiomorphic hammarite ± friedrichite, $Pb_{2.28}Cu_{2.53}Bi_{3.43}Sb_{0.02}S_{8.70}$ (two analyses). Some isolated grains, also embedded in quartz, consist of krupkaite ± lindströmite, $Pb_{1.03}Cu_{1.17}Bi_{2.82}Sb_{0.03}S_{5.95}$ (two analyses) admixed with minor emplectite. Chalcopyrite, pyrite and rare sphalerite complete the primary association of metallic minerals. The first stage of alteration by meteoric water led to the formation of covellite and digenite along cleavages and cracks of pizgrischite or associated sulfosalts. Bismutite and malachite are common and azurite is rare in the second stage of alteration. Some crystals of pizgrischite are completely replaced by a mixture of bismutite and malachite.

Geological setting

Pizgrischite is the main metallic mineral in dm-size pods within a massive to saccaroidal quartz vein (0.5–2 m in thickness) that runs semiparallel to a siderite vein (up to 5 m in thickness; Fig. 1). Both veins can be followed along strike for about 80 m, and are embedded in augen gneisses belonging to the pre-Triassic basement of the Surreta nappe. Similar veins of siderite were actively mined until the second half of the 19th century in Val Ferrera. Grünenfelder (1956) considered the host augen gneiss to be a variety of the early Permian Roffna rhyolite, dated by Marquer *et al.* (1998) at 268.3 ± 0.6 Ma. Marquer *et al.* (1996) suggested that these mineralized augen gneisses represent pre-Carboniferous gneisses that underwent a pre-Alpine high-temperature event. The augen gneiss is overlain by Triassic dolomitic carbonates hosting numerous small stratabound (*i.e.*, Fe–Mn ± As, V, Be, Sb, Mo deposits), which were interpreted to share a syngenetic exhalative origin by Brugger & Gieré (1999, 2000).

Strong silicification is observed in the augen gneiss at the contact of the veins on Piz Grisch (Fig. 1). Both the quartz and siderite veins are discordant relative to the main regional Alpine schistosity (S_1), which formed under greenschist-facies conditions during a complex but still poorly constrained P–T path in the Tertiary, leading from near-blueschist-facies to lower-greenschist-facies conditions (*e.g.,* Baudin *et al.* 1995, Brugger & Gieré 2000). The D_1 episode of folding of the veins and remobilization of siderite in the S_1 foliation unambiguously indicate a pre-D_1 emplacement of the siderite and quartz veins (Fig. 1).

The mineralogy of the siderite veins at Val Ferrera is monotonous, and mostly consists of manganoan siderite and ankerite with accessory hematite. Alkaline skarn-like quartz + green aegirine + hematite or magnetite rocks occur as lenses and layers at the contact between some veins and the hosting gneiss, as lenses within the

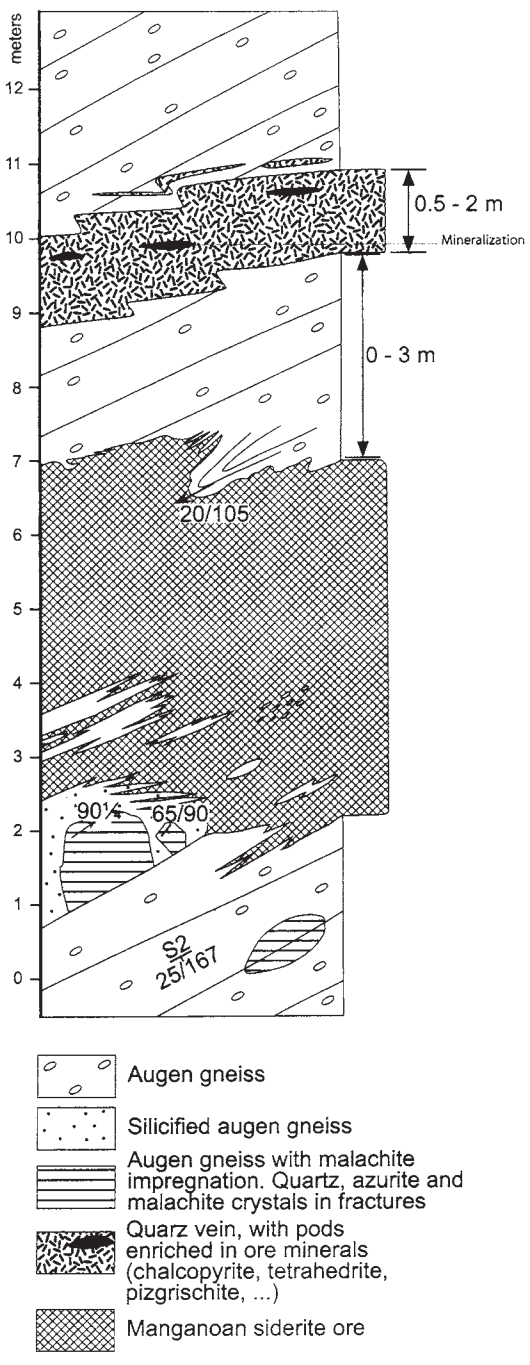

FIG. 1. Synthetic profile through the thickest part of the vein system at Piz Grisch.

ore, or as veinlets cross-cutting the ore; such rocks have not been observed at Piz Grisch. Pyrite and chalcopyrite are rare accessories in the siderite ores.

The quartz vein at Piz Grisch is one of the few pre-Alpine base-metal occurrences known in the Briançonnais domain of the Eastern Swiss Alps. Other occurrences include: 1) stratabound sulfide mineralization (tetrahedrite, chalcopyrite, galena, bornite, pyrite, covellite) in the basal Triassic quartzite at Ursera and Traversa (Surreta nappe, Escher 1935) and in the Triassic marbles near Piz Grisch (Swiss coordinates 754.540/156.060); 2) dolomite – calcite – quartz – barite veinlets with pyrite, uraninite, Se-rich galena, tetrahedrite, sphalerite, chalcopyrite, bornite, covellite, molybdenite in the dolomitic marbles of the Suretta nappe in the hydroelectric tunnel "Valle di Lei – Ferrera" (Dietrich *et al*. 1967) and 3) barite, quartz, carbonate, albite veins with galena, sphalerite, Ag-rich tetrahedrite, chalcopyrite, bornite, pyrite, arsenopyrite, covellite, siegenite, stannite and polybasite–pearceite (Sommerauer 1972) in Mesozoic breccias of the Schams nappe (Escher 1935).

However, the quartz vein at Piz Grisch appears to be unique in Val Ferrera, not only owing to its high Bi-content and mineralogy, but also by its association with a siderite vein. Pizgrischite originated from the remobilization of a primary, pre-Tertiary, hydrothermal quartz–sulfide assemblage during the Alpine regional metamorphism.

Appearance and Physical Properties

The new mineral species occurs as blades up to 1 cm in length. They are metallic lead grey, thin, opaque and striated, forming sprays in quartz (Fig. 2). The poor quality (microfractures, rough surface) and abundant twinning of the crystals chemically extracted from the quartz preclude a complete morphological study. Pizgrischite is brittle, with an uneven fracture, and it possesses a grey-black streak. Cleavage is perfect along {001}, and well developed on {010}; microscopically (Fig. 3), abundant polysynthetic twinning is observed on (010). Vickers micro-indentation hardness, VHN_{100}, measured with a Leitz Durimet (Miniload 2) hardness tester, gave a mean value of 190 and a range of 174–202 kg/mm^2 (n = 10), which corresponds to a Mohs hardness of 3.3(2). These values are comparable to those obtained for the related sulfosalts hodrušhite (200 kg/mm^2; Koděra *et al*. 1970) and kupčíkite (192 kg/mm^2; Topa *et al*. 2003a).

On the basis of the unit-cell volume, 5881.24 Å^3, and using the average result of seven chemical analyses obtained with an electron microprobe, the calculated density D_x is 6.58 g/cm^3.

If observed in reflected light, pizgrischite is not perceptibly bireflectant or pleochroic; it has straight extinction, but is only weakly anisotropic in dark brown. Rotation of the analyzer by a few degrees from full extinction lightens the brown color. In some areas, between crossed polars, irregular lamellae of different shades of brown are perceptible: these may be deformation twins related to late Alpine deformation. Reflectance values in air and oil (Zeiss n_D = 1.515), measured at 23°C from 400 to 700 nm with a Zeiss MPM800 spectrophotometer on a freshly polished grain, are presented in Table 1. As shown in Figure 4, the measured R_{max} values (in air) coincide with those of type hodrušhite from the Rosalia vein, Banská Hodruša, Slovakia (Koděra *et al*. 1970), whereas the R_{max} values (in air) are on average 1.5% higher than those of type kupčíkite from Felbertal, Austria (Topa *et al*. 2003a) and cuprobismutite from Baicolliou, Wallis, Switzerland (Picot & Johan 1977).

Chemical Analyses

Quantitative electron-microprobe analyses of four crystals were carried out with a CAMECA SX 50 instrument. The results are summarized in Table 2, together with operating conditions and the standards used. Pizgrischite is not damaged by the electron beam. The empirical chemical formula, calculated on the basis of 69 atoms per formula unit (*apfu*) from the average results of seven analyses, is: $(Cu_{15.24}Fe_{0.80}Pb_{0.60})_{\Sigma 16.64}$ $(Bi_{17.07}Sb_{0.17})_{\Sigma 17.24}$ $(S_{35.09}Se_{0.03})_{\Sigma 35.12}$.

The resulting imbalance in charges is –0.47 electrons per formula unit, *i.e.,* 0.7% of the negative charges. The simplified formula, in accordance with the crystal-structure refinement reported below, is: (Cu^+,Fe^{2+}) $Cu^+_{14}PbBi_{17}S_{35}$.

X-Ray-Diffraction Study

Preliminary powder diagrams were obtained on a conventional laboratory diffractometer in 1988. As this material turned out to be unsuitable for classical single-crystal X-ray study (Weissenberg and Buerger precession techniques), we decided to wait for better material or technical improvements. The accessibility to XRD powder synchrotron method (European Synchrotron Radiation Facility 2005) and the development of image-plate CCD detectors for single-crystal diffractometers (*e.g.,* Burns 1998) finally enabled us to complete the characterization of this mineral and to solve its crystal structure. Because the mineral cannot be easily distinguished visually from other associated related phases (emplectite and aikinite–bismuthinite-series sulfosalts), each sample used for further studies was first identified by the Gandolfi method.

Powder Diffraction

A quartz-rich sample containing unaltered domains of the new mineral was partially dissolved in 5% aqueous hydrofluoric acid. The pizgrischite crystals were carefully hand-picked from the residue, gently

ground in an agate mortar, and placed in a capillary tube 0.3 mm in diameter, containing about 0.14 mm^3 of powder.

The X-ray synchrotron powder data (Table 3) was measured in Debye–Scherrer geometry, with a distance of 664 mm between the capillary-hosting sample and the receiving slit. Data acquisition was made at the Swiss–Norwegian Beam Line, European Synchrotron Research Facility in Grenoble, with a wavelength λ = 1.09816(1) Å, and a step size of 0.01° 2θ.

The pattern was decomposed into individual intensities using the XND program (Bérar & Baldinozzi 1998) to give a R_{wp} of 0.038. Relative intensities are given with the respect to the strongest line (020). The unit-cell parameters were refined from a Le Bail fit on the powder pattern, using the space group *C*2/*m*. The ensuing lattice parameters and the complete set of powder data are reported in Table 3.

It should be noted that the lattice parameters from the powder are more trustworthy, as they are not biased by the presence of the other twin individual (those from

TABLE 1. REFLECTANCE DATA IN AIR AND OIL OF PIZGRISCHITE

λ (nm)	R_1	R_2	$^{in}R_1$	$^{in}R_2$
400	39.9	40.8	24.80	25.80
420	40.2	41.2	25.00	26.00
440	40.4	41.5	25.05	26.20
460	40.6	42.0	25.20	26.50
470	**40.7**	**42.1**	**25.30**	**26.75**
480	40.8	42.4	25.35	27.00
500	41.0	42.7	25.40	27.15
520	41.1	42.9	25.40	27.25
540	41.1	43.0	25.45	27.40
546	**41.2**	**43.1**	**25.40**	**27.40**
560	41.1	43.1	25.40	27.45
580	41.1	43.1	25.30	27.45
589	**41.2**	**43.3**	**25.40**	**27.50**
600	41.1	43.2	25.30	27.55
620	41.1	43.4	25.25	27.55
640	40.9	43.4	25.05	27.60
650	**40.7**	**43.3**	**25.00**	**27.55**
660	40.5	43.2	24.85	27.50
680	40.3	43.1	24.70	27.30
700	40.1	43.0	24.60	27.15

Measured with a Zeiss MPM800 using a WTiC standard and an oil with n_D = 1.515 at 23 °C. We used ×20 objectives with the same effective numerical aperture of 0.25 for measurements in air and oil.

TABLE 2. COMPOSITION OF PIZGRISCHITE AND FORMULA CALCULATED ON A SUM OF 69 ATOMS

Cu wt.%	16.48	(16.21 - 19.92)	Cu^{1-} *apfu*	15.24
Pb	2.10	(1.70 - 2.56)	Pb^{2-}	0.60
Fe	0.77	(0.74 - 0.80)	Fe^{2-}	0.80
Bi	60.70	(60.10 - 61.62)	Bi^{3-}	17.07
Sb	0.35	(0.26 - 0.47)	Sb^{3-}	0.17
S	19.16	(18.79 - 19.49)	S^{2-}	35.09
Se	0.04	(0.00 - 0.07)	Se^{2-}	0.03
Total	99.60		Total	69.00
			Σ met	33.88
			Cb	-0.47

The composition and range shown are the average result of seven analyses. Data acquired with a CAMECA SX 50 electron microprobe, operated at 20 kV, 15 nA. Dosed element (emission line, standard and standard deviation in wt.%): Cu (*Kα*, synthetic $CuInSe_2$, 0.24), Pb (*Mα*, galena, 0.27), Fe (*Kα*, synthetic FeS, 0.02), Bi (*Mα*, synthetic Bi, 0.47), Sb (*Lα*, stibnite, 0.07), S (*Kα*, galena, 0.25), Se (*Lα*, synthetic Se, 0.02). Elements checked but not detected: Cd, Ag and Te. Zn detected but below standard deviation. Σ met: sum of cations; Cb: charge balance.

FIG. 2. Pizgrischite crystals spray partially altered into malachite (green) and bismutite (yellow) in a fine-grained quartz matrix. Horizontal field of view is 5 cm. Holotype sample MGL #58622. Photo and courtesy S. Ansermet.

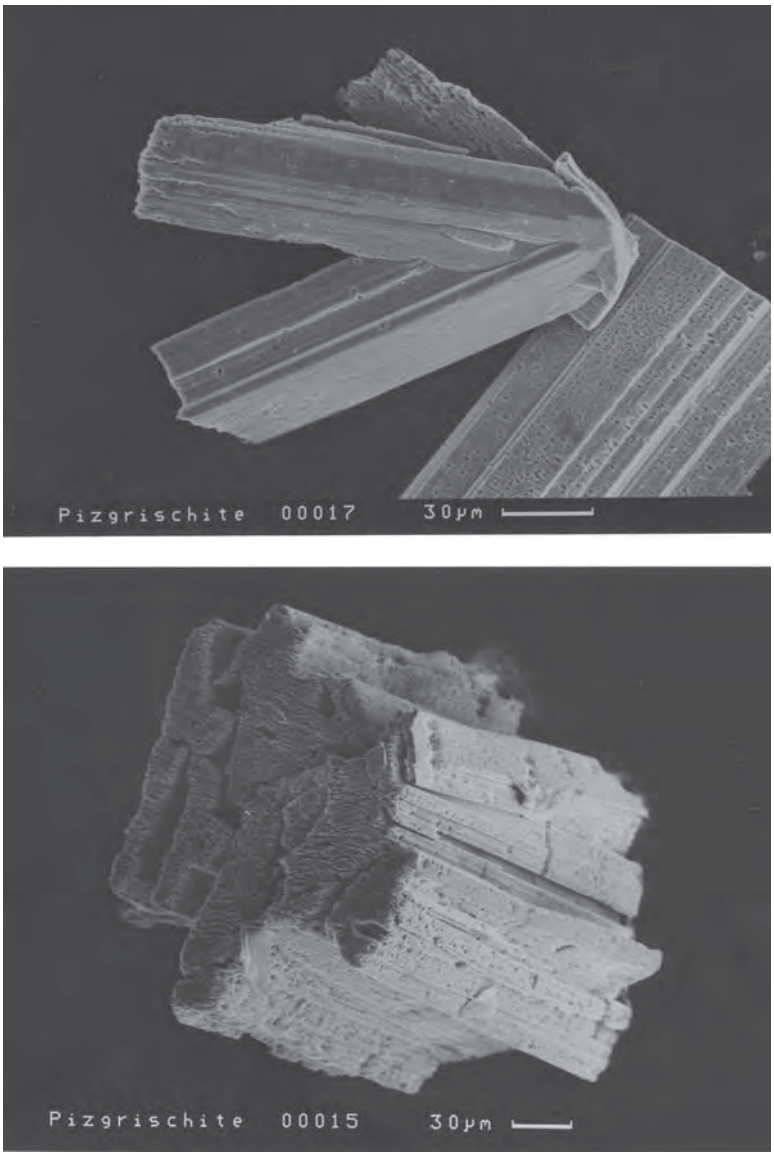

FIG. 3. a, b. SEM images of twinned pizgrischite crystals extracted from quartz matrix by treatment with dilute hydrofluoric acid. Part of holotype sample MGL #58622.

the image-plate data tend toward those from the powder with increasing distance of crystal to image plate).

Structure determination and refinement

The structure of pizgrischite was solved by direct methods (program SHELXS, Sheldrick 1997). An apparently monocrystalline splinter was extracted from a polished section under polarized light (reflecting light microscope). A full hemisphere was collected on a IPDS I instrument equipped with Mo radiation, using the data-collection parameters listed in Table 4. Unfortunately, the measured crystal turned out to be a pseudomerohedral twin. Nevertheless, we were able to determine the unit cell and space group (*C*2/*m*) unequivocally. The reflections from the dominant individual could be integrated, but may contain some contribution from the other individual (this might partly explain the higher

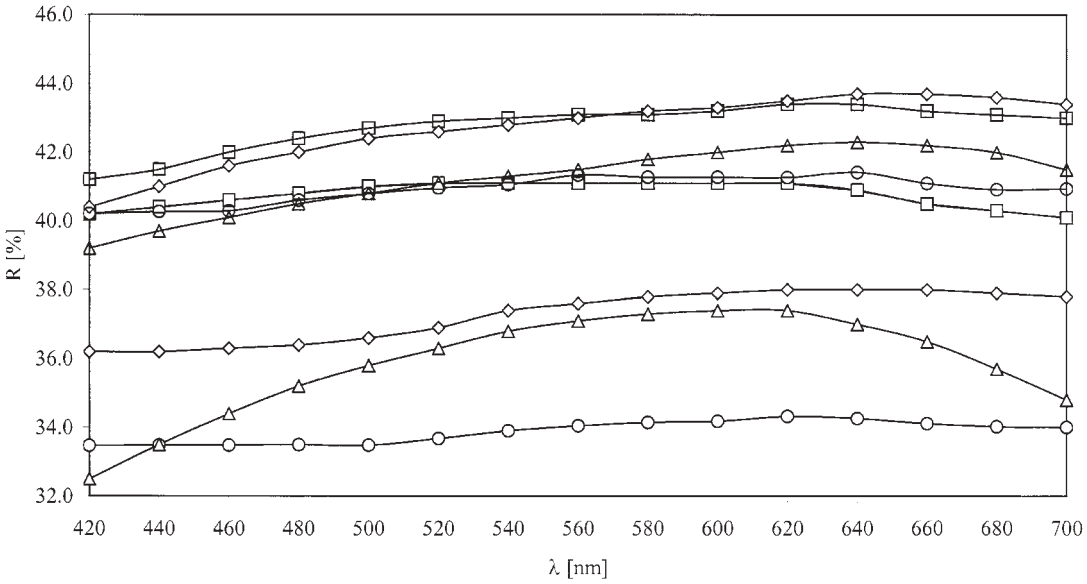

FIG. 4. Maximal and minimal reflectance data in air of pizgrischite (□), compared to those of kupčíkite (○), hodrušhite (◇) and cuprobismutite (△).

than usual R_{int} value). The absorption correction was based on the habit of the measured crystal ({100} and {001} pinacoids, partial {11$\bar{1}$} prism and the (91$\bar{1}$) bevel face). The occupancy of the lead, bismuth and copper atoms was refined anisotropically, whereas the sulfur atoms were treated isotropically. The atom Cu9 required a split position, and the atoms Cu15 and Fe1 occupy the same site: their populations were made to add up to 1.0, and the same *x*, *y* and *z* coordinates as well as the same U_{ij} were imposed on them.

In Table 5, we present the coordinates of the atoms in the structure of pizgrischite, and in Table 6, we list selected interatomic distances. A table of observed and calculated structure-factors is available from the Depository of Unpublished Data on the MAC web site [document Pizgrischite CM45_xxx].

DESCRIPTION OF THE CRYSTAL STRUCTURE

Modular elements

Pizgrischite is related to the cuprobismutite homologous series, as similar structural units occur in pizgrischite and in the cuprobismutite-group minerals. However, pizgrischite does not belong to the cuprobismutite homologues. Three members of the cuprobismutite homologous series are known so far: kupčíkite $Cu_{3.4}Fe_{0.6}Bi_5S_{10}$ (Fig. 5), cuprobismutite $Cu_{10}Bi_{12}S_{23}$ (Fig. 6), and hodrushite $Cu_8Bi_{12}S_{22}$ (not shown here).

The crystal structures of cuprobismutite homologues can be described in terms of regular 1:1 intergrowths on the unit-cell scale of two types of slabs: (a) $(311)_{PbS}$ slabs of a galena-like structure, *i.e.*, kupčíkite-like (simplified in Fig. 5), cuprobismutite-like (Fig. 6) or both (in hodrushite; not shown here), and (b) complex slabs with columns of paired BiS_5 pyramids and CuS_4 coordination tetrahedra (Makovicky 1989, Topa *et al.* 2003b); they are grey-shaded in Figures 5 and 6. The (a) slabs consist of BiS_6 coordination octahedra, coordination pyramids BiS_5 flanking them, and of the fitting parts of the trigonal coordination bipyramids of Cu(Fe). The (b) layers are identical in all homologues, *i.e.*, homologous accretion takes place in the galena-like portions. In kupčíkite, $N = 1$, two coordination pyramids of BiS_5 attach themselves to the appropriate sides of the Bi coordination octahedron (Fig. 5); in cuprobismutite, $N = 2$, there are pairs of such pyramids (Fig. 6). The PbS-like slab is then two and three octahedra (or pyramids) wide, respectively (Figs. 5, 6). Hodrushite is a regular 1:1 combination of these two slab thicknesses, $N = 1, 2$ (Topa *et al.* 2003b).

The principle of the pizgrischite structure can be compared to that of sartorite homologues. In modular description, the sartorite homologues are composed of slices of SnS-like structure cut parallel to $(301)_{SnS}$ or $(30\bar{1})_{SnS}$. Similarly, the pizgrischite structure is composed of slices of kupčíkite-like structure cut parallel to $(201)_{kpk}$ (Fig. 5). In the sartorite homo-

TABLE 3. POWDER X-RAY-DIFFRACTION DATA AND LATTICE PARAMETERS REFINED FROM *d* VALUES FOR PIZGRISCHITE

h	*k*	*l*	*d*	I/I_{max} calc	*d*	I/I_{max} meas	*h*	*k*	*l*	*d*	I/I_{max} calc	*d*	I/I_{max} meas
2	0	4	8.696	1	8.696	2	$\bar{6}$	0	15	2.693	15	2.693	14
0	0	5	8.578	3	8.578	3	$\bar{9}$	1	5	2.685	18	2.686	17
$\bar{4}$	0	3	7.852	10	7.842	9	$\bar{8}$	0	14	2.656	4	2.656	9
$\bar{4}$	0	4	7.181	13	7.157	29	3	1	11	2.639	10	2.639	9
$\bar{4}$	0	5	6.501	7	6.501	5	$\bar{3}$	1	12	2.623	7	2.622	9
4	0	4	6.402	3	6.396	3	1	1	12	2.614	6	2.615	11
0	0	7	6.129	6	6.129	3	5	1	10	2.598	44	2.597	34
$\bar{4}$	0	6	5.873	3	5.862	2	7	1	8	2.588	5	2.588	13
4	0	5	5.781	2	5.802	10	9	1	5	2.558	3	2.557	4
6	0	2	5.443	2	5.443	3	$\bar{5}$	1	12	2.542	36	2.541	38
$\bar{6}$	0	4	5.373	20	5.364	40	$\bar{3}$	1	13	2.512	1	2.511	3
6	0	3	5.171	2	5.176	2	7	1	9	2.503	3	2.502	8
$\bar{4}$	0	8	4.825	5	4.825	4	$\bar{9}$	1	9	2.473	7	2.473	7
4	0	7	4.756	2	4.759	4	2	0	17	2.457	4	2.457	8
$\bar{6}$	0	7	4.483	17	4.483	12	11	1	1	2.444	7	2.446	7
2	0	9	4.467	6	4.464	6	14	0	2	2.438	2	2.439	7
$\bar{4}$	0	9	4.405	4	4.402	3	$\bar{6}$	0	17	2.420	3	2.420	24
8	0	0	4.354	2	4.351	5	1	1	14	2.391	5	2.394	4
$\bar{2}$	0	10	4.283	2	4.283	4	10	0	12	2.360	3	2.361	6
$\bar{8}$	0	4	4.209	2	4.207	2	4	0	17	2.351	2	2.351	6
$\bar{6}$	0	8	4.190	3	4.190	4	7	1	11	2.334	4	2.334	7
$\bar{8}$	0	5	4.080	28	4.080	50	$\bar{1}$	1	15	2.318	3	2.597	4
2	0	10	4.056	4	4.059	5	$\bar{3}$	1	15	2.307	3	2.305	6
8	0	3	4.036	3	4.036	5	12	0	10	2.282	4	2.282	4
6	0	7	3.987	15	3.987	22	$\bar{9}$	1	12	2.274	11	2.273	16
$\bar{2}$	0	11	3.904	25	3.904	37	$\bar{7}$	1	14	2.253	2	2.254	4
8	0	4	3.878	5	3.878	15	5	1	14	2.217	7	2.217	12
1	1	2	3.817	4	3.815	4	$\bar{8}$	0	18	2.202	10	2.201	8
$\bar{1}$	1	3	3.763	1	3.763	3	7	1	13	2.172	11	2.172	23
3	1	0	3.708	17	3.708	34	11	1	8	2.163	4	2.163	9
$\bar{3}$	1	2	3.676	4	3.674	10	13	1	3	2.153	10	2.152	8
1	1	4	3.640	18	3.640	15	0	0	20	2.145	14	2.146	11
$\bar{2}$	0	12	3.585	31	3.585	34	$\bar{1}$	1	17	2.129	15	2.129	18
0	0	12	3.575	9	3.575	11	13	1	4	2.124	11	2.124	21
3	1	3	3.557	3	3.557	7	6	0	18	2.119	15	2.119	17
1	1	5	3.524	16	3.524	10	1	1	17	2.104	11	2.105	10
$\bar{3}$	1	5	3.451	10	3.451	15	10	0	15	2.094	2	2.094	9
2	0	12	3.425	19	3.425	31	8	0	17	2.080	12	2.080	7
8	0	7	3.367	20	3.367	19	$\bar{9}$	1	15	2.070	7	2.070	6
$\bar{3}$	1	6	3.342	3	3.341	8	3	1	17	2.051	13	2.051	21
$\bar{2}$	0	13	3.315	8	3.313	9	$\bar{1}$	1	18	2.044	1	2.044	2
10	0	3	3.296	24	3.294	15	7	1	17	2.023	4	2.023	8
$\bar{3}$	1	5	3.234	16	3.232	16	1	1	18	2.020	4	2.020	8
10	0	4	3.203	19	3.203	29	10	0	16	2.013	10	2.013	11
4	0	12	3.179	23	3.179	27	$\bar{5}$	1	18	2.009	15	2.007	15
$\bar{3}$	1	6	3.150	26	3.148	23	$\bar{9}$	1	16	2.005	13	2.003	20
1	1	8	3.128	6	3.120	40	11	1	11	2.001	14	1.999	20
$\bar{3}$	1	8	3.104	23	3.104	68	15	1	0	1.996	10	1.995	11
$\bar{7}$	1	1	3.083	12	3.083	32	$\bar{3}$	1	19	1.961	11	1.960	2
7	1	0	3.075	5	3.075	31	0	2	0	1.956	100	1.956	100
7	1	1	3.052	12	3.052	26	0	2	2	1.948	14	1.949	28
8	0	9	3.042	10	3.043	12	$\bar{9}$	1	17	1.942	6	1.942	25
7	1	2	3.013	5	3.013	15	15	1	4	1.928	3	1.928	7
3	1	8	2.998	18	2.998	28	2	2	3	1.923	4	1.923	8
$\bar{3}$	1	9	2.981	21	2.981	18	15	1	5	1.902	5	1.902	12
7	1	3	2.963	7	2.963	15	2	2	5	1.890	3	1.890	7
$\bar{8}$	0	12	2.936	3	2.936	4	$\bar{1}$	1	20	1.888	3	1.888	9
7	1	4	2.901	8	2.901	23	$\bar{9}$	1	18	1.880	5	1.880	7
10	0	7	2.885	11	2.884	13	0	0	23	1.865	4	1.865	11
3	1	9	2.875	19	2.874	28	$\bar{6}$	2	3	1.847	4	1.847	10
$\bar{3}$	1	10	2.858	5	2.857	13	0	2	8	1.838	4	1.838	8
$\bar{5}$	1	9	2.852	13	2.852	16	7	1	18	1.821	3	1.821	7
7	1	5	2.831	21	2.829	30	$\bar{1}$	1	21	1.818	1	1.817	5
5	1	8	2.806	16	2.806	12	17	1	0	1.814	5	1.814	12
$\bar{8}$	0	13	2.791	9	2.791	13	17	1	2	1.792	3	1.792	6
$\bar{1}$	1	11	2.772	12	2.772	15	6	0	22	1.786	2	1.786	16
$\bar{9}$	1	1	2.760	42	2.759	53	17	1	3	1.777	4	1.777	7
9	1	0	2.751	14	2.752	44	16	0	12	1.769	1	1.769	4
9	1	2	2.700	10	2.701	19							

Lattice parameters refined from *d* values: *a* 35.054(2), *b* 3.91123(1), *c* 43.192(2) Å, β 96.713(4)°, *V* 5881.24 Å^3. Diffractometer with Debye–Scherrer geometry, 1.328 m diameter. Synchrotron X-ray radiation, wavelength λ 1.09816(1) Å, step size of 0.01° 2θ. Selected data on the basis of I/I_{max} (meas.) > 1.

logues, the known slab-widths are exclusively three and four square coordination pyramids if measured diagonally along $[001]_{SnS}$. In pizgrischite, similar counting units are missing. An attempt is made here to use the number of "unbroken" columns of paired BiS_5 pyramids and CuS_4 coordination tetrahedra in the thin layers measured diagonally along $[100]_{kpk}$ (Fig. 5). In doing so, the structure of pizgrischite (Fig. 7) can be described as composed of slices of a kupčíkite-like structure cut parallel to $(201)_{kpk}$ (Fig. 5). The slabs are five and seven columns thick, respectively, and alternate along $[001]_{pgr}$. They are symmetry-related to each other by rotation around a two-fold axis $[203]_{kpk}$. Along the composition zone $(001)_{pgr}$, the slabs apparently transform into cuprobismutite, as described in the following section. Thus, pizgrischite can be considered the first known homologue $N = 5, 7$ of a possible pizgrischite homologous series.

TABLE 4. SINGLE-CRYSTAL X-RAY-DIFFRACTION DATA CONCERNING PIZGRISCHITE AND EXPERIMENTAL DETAILS

Crystal data

Chemical formula	$(Cu,Fe)Cu_{14}PbBi_{17}S_{35}$	Formula weight	5891.04
Cell setting	Monoclinic	Space group	*C*2/*m*
a (Å)	35.095(7)	*b* (Å)	3.9067(8)
c (Å)	43.222(9)	β (°)	96.71(3)°
V (Å^3)	5885(2)	*Z*	4
D_x (g/cm^3)	6.58	Radiation type	Mo*K*α
Wavelength (Å)	0.71073		
No. of reflections for cell parameters	1523	Temperature (K)	293
		μ (mm^{-1})	59.885
Crystal form	platelet	Crystal size (mm)	0.090 × 0.150 × 0.190
Crystal color	metallic grey		

Data collection

Absorption correction: numerical			
T_{min}	0.0132	T_{max}	0.0963
No. of measured reflections	12204	No. of independent reflections	3625
No. of observed reflections	3270	Criterion for observed reflections	$I > 2\sigma(I)$
R_{int}	0.0946	θ_{max} (°)	20.86
Range of *h*	-34 < *h* < 34	Range of *k*	-3 < *k* < 3
Range of *l*	-43 < *l* < 43	Full hemisphere	
Data collection: Stoe IPDS–I			

Refinement

Refinement on F_o^2		R [$> 2\sigma(F_o^2)$]	6.11%
$wR(F_o^2)$	16.45%	*S* (*GooF*)	1.064
No. of reflections used in refinement	3625	No. of parameters refined	307
$(\Delta/\sigma)_{max}$	0.002	Δ_{max} (e/Å^3)	4.74
$\Delta\rho_{min}$ (e/Å^3)	-3.67	Extinction correction	none

Weighting scheme $w = 1/[\sigma^2(F_o^2) + (0.1199P)^2 + 316.6955P]$, where $P = (F_o^2 + 2F_c^2)/3$. Scattering factors from International Tables for Crystallography (Vol. C)

Computer programs

Program used to solve structure: SHELXS97 (Sheldrick 1997)
Program used to refine structure: SHELXL97 (Sheldrick 1997)

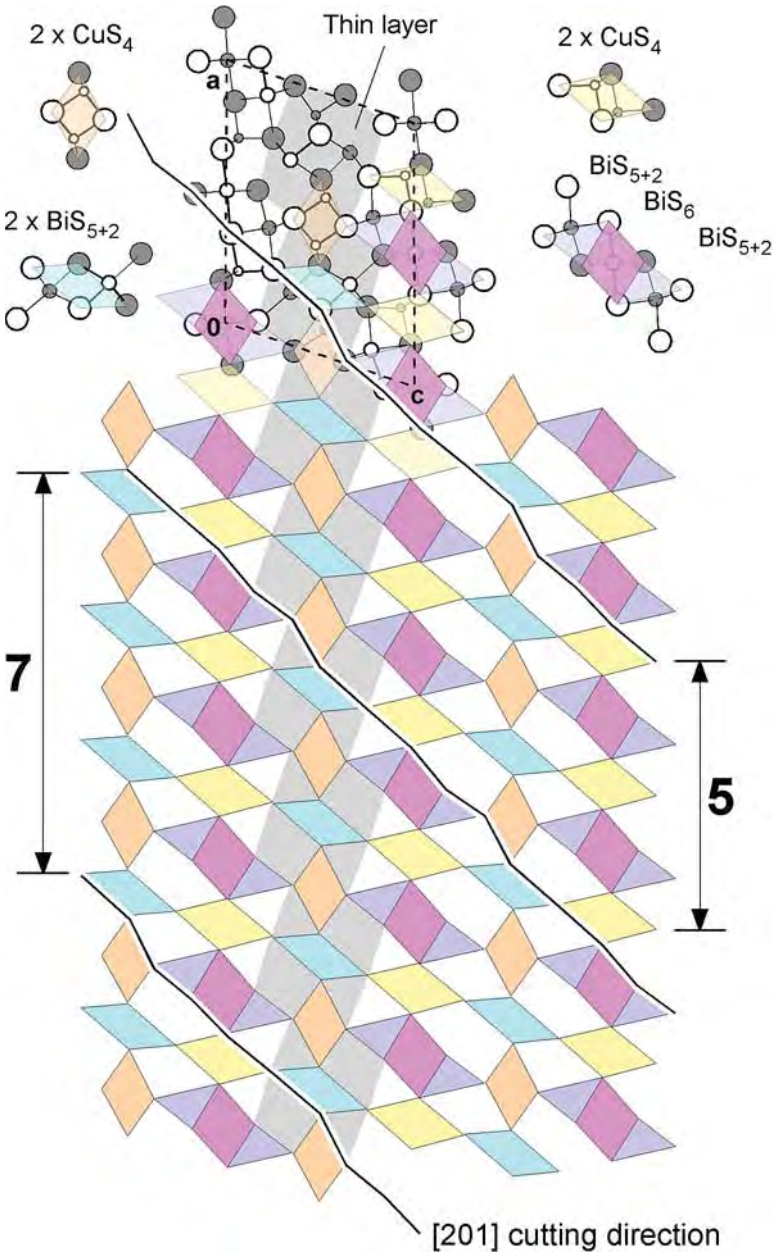

FIG. 5. Crystal structure of kupčíkite projected along [0$\bar{1}$0]. Small, medium and large circles indicate Cu, Bi, and S atoms, respectively. The white and grey colors indicate a relative difference in height of about 2 Å. Four different clusters of Cu–S and Bi–S polyhedra are shown consisting of CuS_4: tetrahedron, BiS_6: octahedron, BiS_5: square pyramid (completed by two additional atoms of S into BiS_{5+2}: monocapped trigonal prism). Gray shading indicates the b slab of cuprobismutite homologues (thin layer). A tiling pattern is derived from the clusters and a thin layer according to Topa *et al*. (2003a) is shown. Two slabs, five and seven columns thick, and the corresponding cutting direction $[201]_{kpk}$, are illustrated. These slabs are the basic building units of the pizgrischite structure. Details are provided in the text.

TABLE 5. ATOM PARAMETERS FOR PIZGRISCHITE

Atom	*x*	*y*	*z*	*BVC*	U_{11}	U_{22}	U_{33}	U_{13}	U_{eq}
Pb1	0.87808(5)	1/2	0.28981(4)	1.88	0.0262(9)	0.0493(13)	0.0350(9)	-0.0040(7)	0.0374(6)
Bi1	0.83272(4)	1/2	0.43024(3)	3.25	0.0107(8)	0.0149(10)	0.0292(9)	-0.0029(6)	0.0187(5)
Bi2	0.43533(4)	1/2	0.43755(3)	3.25	0.0112(8)	0.0190(10)	0.0299(9)	-0.0042(6)	0.0206(5)
Bi3	0.48725(4)	1/2	0.29006(3)	3.15	0.0143(8)	0.0142(9)	0.0301(8)	-0.0057(6)	0.0202(5)
Bi4	0.22486(4)	1/2	0.41883(3)	3.10	0.0121(8)	0.0172(9)	0.0291(8)	-0.0027(6)	0.0199(5)
Bi5	0.54122(4)	1/2	0.39190(3)	3.07	0.0116(8)	0.0172(9)	0.0273(8)	-0.0043(6)	0.0192(5)
Bi6	0.77605(4)	1/2	0.33146(3)	2.97	0.0141(8)	0.0280(11)	0.0326(9)	-0.0058(6)	0.0256(5)
Bi7	0.07211(4)	1/2	0.10866(3)	3.07	0.0142(8)	0.0191(10)	0.0255(8)	-0.0051(6)	0.0202(5)
Bi8	0.11792(4)	1/2	0.46427(3)	2.99	0.0148(8)	0.0207(10)	0.0288(8)	-0.0046(6)	0.0220(5)
Bi9	0.29783(4)	1/2	0.15429(3)	3.12	0.0127(8)	0.0146(9)	0.0291(8)	-0.0056(6)	0.0194(5)
Bi10	0.35170(4)	1/2	0.06782(3)	3.12	0.0149(8)	0.0144(9)	0.0294(8)	-0.0009(6)	0.0198(5)
Bi11	0.62900(4)	1/2	0.03831(3)	2.99	0.0113(8)	0.0188(9)	0.0281(8)	-0.0049(6)	0.0200(5)
Bi12	0.09069(4)	1/2	0.29255(3)	3.02	0.0171(8)	0.0197(10)	0.0307(9)	-0.0054(7)	0.0231(5)
Bi13	0.71726(4)	1	0.25356(3)	3.10	0.0246(9)	0.0201(10)	0.0283(9)	-0.0071(7)	0.0251(5)
Bi14	0.95322(4)	1/2	0.06212(3)	3.17	0.0125(8)	0.0206(10)	0.0287(8)	-0.0024(6)	0.0210(5)
Bi15	0.40889(4)	1/2	0.20603(3)	3.23	0.0136(8)	0.0153(9)	0.0276(8)	-0.0064(6)	0.0195(5)
Bi16	0.11495(4)	1/2	0.20713(3)	3.14	0.0121(8)	0.0218(10)	0.0304(8)	-0.0031(6)	0.0219(5)
Bi17	0.74597(4)	1/2	0.07344(3)	3.08	0.0115(8)	0.0307(10)	0.0305(9)	-0.0059(6)	0.0249(5)
Cu1	0.81357(12)	1/2	0.23153(11)	1.21	0.017(2)	0.028(3)	0.039(3)	-0.004(2)	0.0286(16)
Cu2	0.53261(13)	1/2	0.03173(12)	2.12	0.017(3)	0.026(3)	0.048(3)	-0.011(2)	0.0315(17)
Cu3	0.63631(13)	1/2	0.38674(13)	1.20	0.022(3)	0.024(3)	0.057(3)	0.007(2)	0.0341(17)
Cu4	0.28162(13)	1/2	0.49869(12)	1.27	0.028(3)	0.025(3)	0.041(3)	-0.012(2)	0.0326(17)
Cu5	0.70395(12)	1/2	0.18146(12)	1.22	0.014(2)	0.019(3)	0.048(3)	0.002(2)	0.0271(16)
Cu6	0.94277(15)	1/2	0.35623(13)	1.18	0.038(3)	0.026(3)	0.049(3)	-0.022(3)	0.0398(17)
Cu7	0.16616(12)	1/2	0.12222(11)	1.65	0.016(2)	0.030(3)	0.035(3)	-0.005(2)	0.0276(16)
Cu8	0.02411(13)	1/2	0.46870(12)	1.24	0.026(3)	0.026(3)	0.043(3)	0.007(2)	0.0314(17)
*Cu9A	0.6811(4)	1/2	0.3236(4)	1.25	0.029(5)	0.029(5)			
*Cu9B	0.6724(3)	1/2	0.3071(3)	1.16	0.027(4)	0.027(4)			
Cu10	0.48048(15)	1/2	0.14103(13)	1.13	0.030(3)	0.075(5)	0.046(3)	-0.002(3)	0.051(2)
Cu11	0.9185(2)	1/2	0.13739(15)	1.16	0.090(5)	0.021(4)	0.064(4)	0.045(4)	0.055(3)
Cu12	0.00502(15)	1/2	0.22807(12)	1.02	0.041(3)	0.029(3)	0.042(3)	-0.013(2)	0.0387(17)
Cu13	0.37489(16)	1/2	0.36494(12)	1.19	0.051(3)	0.023(3)	0.041(3)	-0.027(3)	0.0409(17)
Cu14	0.52719(15)	1/2	0.19096(13)	1.06	0.028(3)	0.088(5)	0.046(3)	0.001(3)	0.054(2)
*Cu15/Fe1	0.78546(17)	1/2	0.00309(12)	1.14	0.062(4)	0.025(3)	0.033(3)	0.012(3)	0.0395(19)
S1	0.6732(2)	1	0.17639(19)	2.22	0.016(2)				
S2	0.3297(3)	1/2	0.5389(2)	2.01	0.019(2)				
S3	0.2879(2)	1/2	0.3929(2)	2.10	0.018(2)				
S4	0.1087(2)	1/2	0.40303(19)	2.01	0.014(2)				
S5	0.5516(2)	1/2	0.45275(19)	2.10	0.015(2)				
S6	0.7687(2)	1/2	0.1869(2)	2.16	0.018(2)				
S7	0.9899(3)	1/2	0.3965(2)	2.12	0.019(2)				
S8	0.6559(3)	1/2	0.2509(2)	1.89	0.018(2)				
S9	0.5827(2)	1/2	0.16938(19)	2.08	0.015(2)				
S10	0.0303(3)	1/2	0.3229(2)	2.22	0.018(2)				
S11	0.5404(3)	1/2	0.2453(2)	1.75	0.020(2)				
S12	0.8734(2)	1/2	0.17144(19)	2.13	0.013(2)				
S13	0.7113(2)	1	0.31240(19)	2.77	0.013(2)				
S14	0.6827(2)	0	0.03947(19)	2.13	0.014(2)				
S15	0.3280(2)	1/2	0.3240(2)	2.13	0.017(2)				
S16	0.8818(2)	1/2	0.0335(2)	2.17	0.018(2)				
S17	0.6167(3)	1/2	0.3301(2)	2.59	0.019(2)				
S18	0.5185(2)	1/2	0.10135(19)	2.04	0.016(2)				
S19	0.4292(2)	1/2	0.32849(19)	1.92	0.016(2)				
S20	0.7723(3)	1/2	0.4705(2)	1.61	0.022(2)				
S21	0.4661(2)	1/2	0.0239(2)	2.27	0.017(2)				

S22	0.9842(3)	1/2	0.1742(2)	1.38	0.021(2)
S23	0.7008(3)	1/2	0.3805(2)	2.30	0.017(2)
S24	0.8150(2)	1/2	0.10498(19)	2.35	0.016(2)
S25	0.2815(2)	1/2	0.0320(2)	1.96	0.016(2)
S26	0.6373(3)	1/2	0.0991(2)	1.97	0.019(2)
S27	0.7715(2)	1/2	0.2687(2)	2.30	0.017(2)
S28	0.9593(3)	1/2	0.4757(2)	2.29	0.018(2)
S29	0.3516(2)	1/2	0.23875(19)	2.10	0.016(2)
S30	0.8875(2)	1/2	0.3925(2)	2.05	0.016(2)
S31	0.0662(3)	1/2	0.0475(2)	2.07	0.021(2)
S32	0.4209(3)	1/2	0.1095(2)	1.86	0.024(2)
S33	0.9440(3)	1/2	0.2524(2)	2.11	0.021(2)
S34	0.3728(2)	1/2	0.46547(19)	2.20	0.016(2)
S35	0.2321(3)	1/2	0.1151(2)	2.27	0.019(2)

Notes: Site-occupancy factors fixed to unity, except (*) Cu9A: Cu 0.43(6), Cu9B: Cu 0.57(6), Cu15: Cu 0.77(10), Fe 0.23(10). For all atoms $U_{12} = U_{23} = 0$ by symmetry. BVC: bond-valence calculation.

Tiles and tiling patterns

In order to better understand how the structure of pizgrischite is derived from that of the cuprobismutite homologues, it is necessary to further decompose the above-introduced $N = 5$ and $N = 7$ slabs (modules) into submodular clusters of coordination polyhedra. It is then possible to use the projection of these clusters and to describe the structure in terms of tiling patterns.

Figure 5 shows the structure of kupčíkite and the tiles derived from it: in the (a) slab (*cf.* previous section), pairs of CuS_4 tetrahedra are represented by yellow rhombi, and the BiS_6 octahedra as pink rhombi flanked by the BiS_5 pyramids indicated as mauve triangles; in the (b) slabs ("thin layers"), pairs of CuS_4 tetrahedra are represented by beige rhombi, and the pairs of BiS_5 pyramids as turquoise rhombi. The four individual tiles and their composition as tiling pattern are shown. One thin layer is shaded in grey. In addition, the cutting direction [201] and two slabs, $N = 5$ and $N = 7$, are shown.

Figure 6 shows the structure of cuprobismutite and the tiles derived from it: in the (a) slabs, CuS_4 tetrahedra are represented by yellow triangles, and the BiS_6 octahedra as pink rhombi flanked by the pairs of BiS_5 pyramids indicated as mauve rhombi; the (b) slabs are identical to those in Figure 5. The four individual tiles and their composition as a tiling pattern as well as one grey-shaded thin layer are shown.

Figure 7 shows the structure of pizgrischite. We show the (001) composition zones of the $N = 5$ and $N = 7$ slabs in dark grey, and the thin layers within the kupčíkite-like slabs in light grey. A herringbone-like pattern becomes clearly visible. The small unit-cell of kupčíkite is indicated, and a comparison with Figure 5 shows the identity of the two sections of the structure. The colored tiles underline this aspect. It is very interesting to observe the lateral transformation of the kupčíkite-like slabs into cuprobismutite in, or close to, the composition zone. As real hinges connecting the $N = 5$ and $N = 7$ slabs serve the $Cu(1)S_4$ tetrahedra (beige triangles within the dark grey-shaded composition zones; Fig. 7): they can be interpreted either as a continuation of the kupčíkite-like tiling pattern (if looking at the $N = 7$ slab) or part of the cuprobismutite-like tiling pattern (if looking at the $N = 5$ slab).

If one looks close to the tiles of pizgrischite, one can see that they are more distorted compared to those of kupčíkite and cuprobismutite. This aspect is discussed further in the next section in the context of individual coordination-polyhedra.

Coordination polyhedra

The Bi sites. In cuprobismutite homologues, Topa *et al*. (2003a) distinguished two types of BiS_6 octahedra: unsubstituted and substituted ones. In pizgrischite (Fig. 7), only unsubstituted BiS_6 octahedra are present (Bi1; Bi3, Bi10). As described above, BiS_5 pyramids (and one PbS_5 pyramid) flank the BiS_6 octahedra on appropriate sides (Fig. 7): $Bi(4)S_5$–$Bi(1)S_6$–$Bi(2)S_6$, $Pb(1)S_5$–$Bi(3)S_6$–$Bi(12)S_6$, $Bi(14)S_5$–$Bi(10)S_6$–$Bi(17)S_6$. As in kupčíkite, the coordination polyhedra of all flanking BiS_5 pyramids is completed by two distant S atoms. Thus, for example, $Bi(4)S_5$ can alternatively be described as $Bi(4)S_{5+2}$, a monocapped trigonal prism. In cuprobismutite, however, these flanking BiS_5 pyramids are each completed by one additional S atom into distorted BiS_6 octahedra. In, or close to, the domain zone $(001)_{pgr}$, kupčíkite transforms into cuprobismutite by attaching monocapped trigonal prisms $Bi(15)S_{5+2}$ to $Pb(1)S_{5+2}$ and $Bi(9)S_{5+2}$ to $Bi(17)S_{5+2}$, respectively (Fig. 7). It is very interesting to observe that $Pb(1)S_{5+2}$ and $Bi(17)S_{5+2}$ retain their original coordination (kupčíkite-like, *i.e.,* monocapped trigonal prisms) and

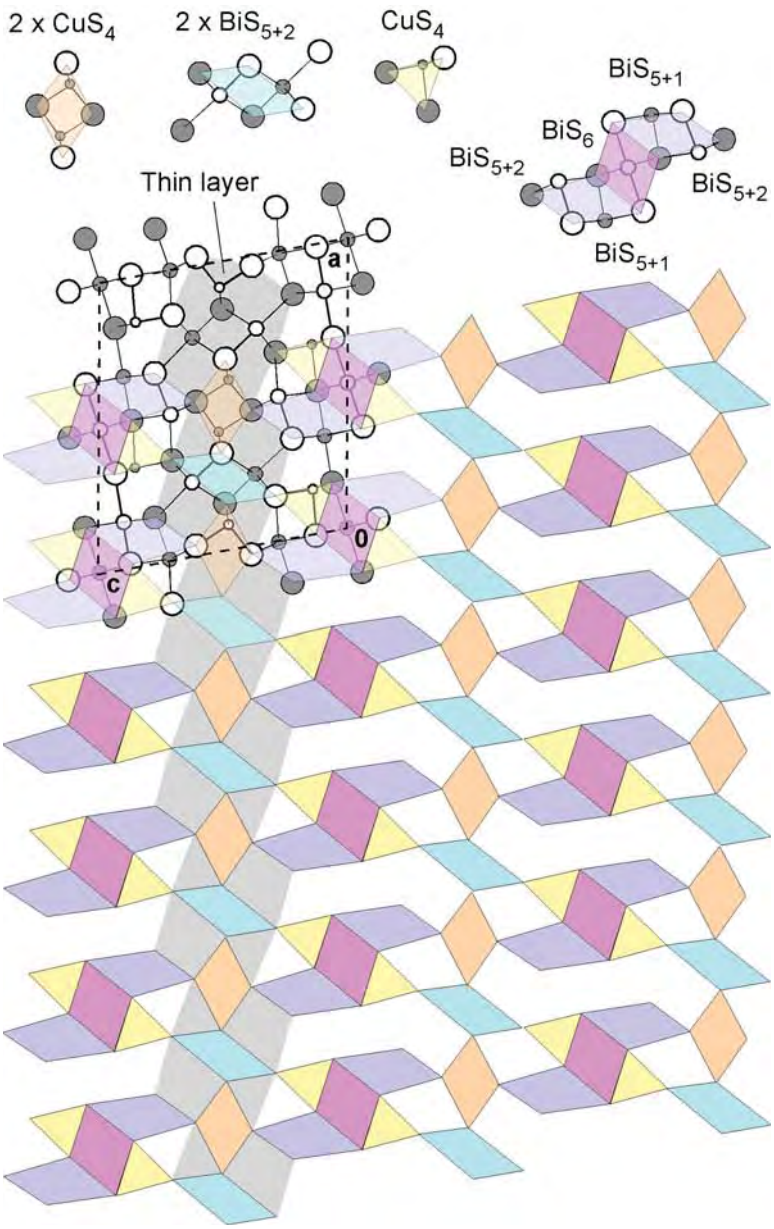

FIG. 6. Crystal structure of cuprobismutite projected along [010]. Small, medium and large circles indicate Cu, Bi, and S atoms, respectively. The white and grey colors indicate a relative difference in height of about 2 Å. Four different clusters of Cu–S and Bi–S polyhedra are shown (*cf.* caption of Fig. 5; BiS_{5+1}: octahedron) and a tiling pattern is derived as well. A thin layer, identical to the one in Figure 5, is shown. Details are provided in the text.

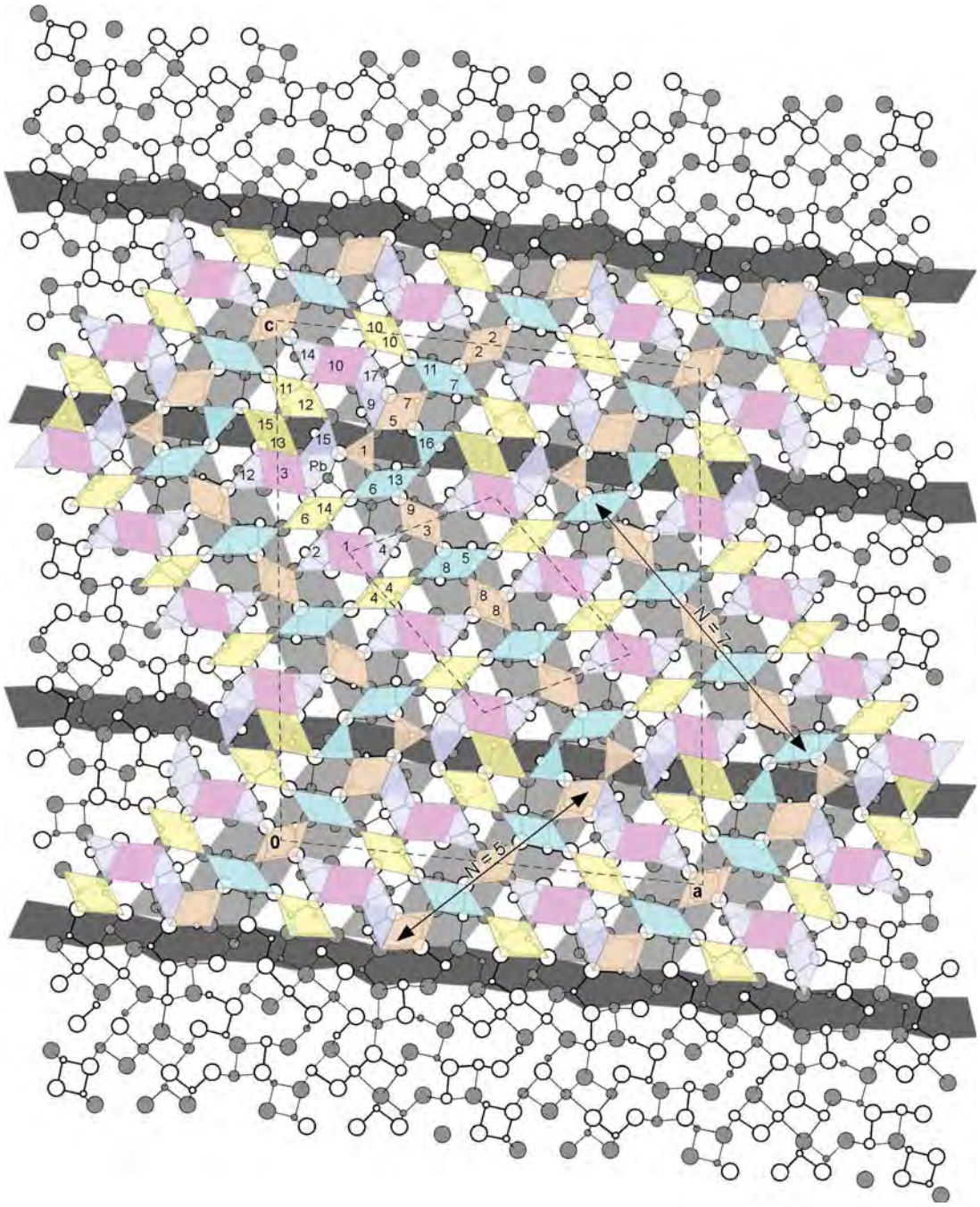

FIG. 7. Crystal structure of pizgrischite projected along [010]. Small, medium and large circles indicate Cu, Bi (Pb), and S atoms, respectively. The white and grey colors indicate a relative difference in height of about 2 Å. Dark grey shaded bands indicate the composition zones of the slices of kupčíkite-like structure (small unit-cell) cut parallel to $(201)_{kpk}$. The thin layers of kupčíkite are shown in light grey (*cf.* Fig. 5) and underline the herringbone-like pattern of the pizgrischite structure.

TABLE 6. SELECTED INTERATOMIC DISTANCES IN PIZGRISCHITE

Pb1–S33	2.996(9)	Bi6–S15ii	2.716(6)	Bi12–S17iii	2.634(6)	Cu3–S4ii	2.325(5)	Cu10–S22iv	2.418(6)
Pb1–S29i	3.012(6)	Bi6–S15i	2.716(6)	Bi12–S17iv	2.634(6)	Cu3–S17	2.463(10)	Cu10–Cu14	2.553(8)
Pb1–S29ii	3.012(6)	Bi6–S13v	3.037(6)	Bi13–S13	2.576(8)	Cu4–S2	2.278(10)	Cu10–Cu11iv	2.915(6)
Pb1–S19ii	3.026(7)	Bi6–S13	3.037(6)	Bi13–S27	2.753(6)	Cu4–S20iv	2.305(5)	Cu10–Cu11iii	2.915(6)
Pb1–S19i	3.026(7)	Bi6–Cu9A	3.310(13)	Bi13–S27viii	2.753(6)	Cu4–S20iii	2.305(5)	Cu11–S12	2.283(10)
Pb1–S15i	3.114(7)	Bi7–S31	2.629(9)	Bi13–S8viii	2.900(7)	Cu4–S20x	2.436(10)	Cu11–S32i	2.302(6)
Pb1–S15ii	3.114(7)	Bi7–S18iv	2.705(6)	Bi13–S8	2.901(7)	Cu4–Cu4vii	2.969(7)	Cu11–S32ii	2.302(6)
Pb1–Cu1	3.184(5)	Bi7–S18iii	2.705(6)	Bi14–S21i	2.630(6)	Cu4–Cu4vi	2.969(7)	Cu11–S22	2.646(12)
Bi1–S30	2.662(8)	Bi7–S26iii	3.074(7)	Bi14–S21ii	2.630(6)	Cu5–S1v	2.229(5)	Cu11–Cu10ii	2.915(6)
Bi1–S34ii	2.759(6)	Bi7–S26iv	3.074(7)	Bi14–S16	2.664(9)	Cu5–S1	2.229(5)	Cu11–Cu10i	2.915(6)
Bi1–S34i	2.759(6)	Bi7–Cu7	3.284(5)	Bi15–S29	2.591(8)	Cu5–S6	2.258(10)	Cu12–S22xi	2.357(10)
Bi1–S3i	2.882(6)	Bi8–S4	2.629(8)	Bi15–S12iv	2.678(6)	Cu6–S7	2.256(10)	Cu12–S11iii	2.387(6)
Bi1–S3ii	2.882(6)	Bi8–S2vi	2.696(6)	Bi15–S12iii	2.678(6)	Cu6–S19i	2.313(5)	Cu12–S11iv	2.387(6)
Bi1–S20	2.898(9)	Bi8–S2vii	2.696(6)	Bi15–S33iii	2.963(7)	Cu6–S19ii	2.313(5)	Cu12–S33xi	2.495(10)
Bi2–S34	2.625(9)	Bi8–S5iv	3.035(6)	Bi15–S33iv	2.963(7)	Cu6–S30	2.633(10)	Cu12–Cu14iv	2.699(5)
Bi2–S28iii	2.631(6)	Bi8–S5iii	3.035(6)	Bi16–S1iv	2.566(8)	Cu7–S1iv	2.325(10)	Cu12–Cu14iii	2.699(5)
Bi2–S28iv	2.631(6)	Bi8–Cu8	3.321(5)	Bi16–S9iv	2.707(6)	Cu7–S26iv	2.367(6)	Cu13–S15	2.273(10)
Bi2–S30iv	3.107(7)	Bi9–S6iii	2.680(6)	Bi16–S9iii	2.707(6)	Cu7–S26iii	2.367(6)	Cu13–S30iii	2.305(5)
Bi2–S30iii	3.107(7)	Bi9–S6iv	2.680(6)	Bi16–S8iii	2.971(7)	Cu7–S35	2.371(10)	Cu13–S30iv	2.305(5)
Bi3–S10ii	2.759(6)	Bi9–S35	2.696(9)	Bi16–S8iv	2.971(7)	Cu8–S5iii	2.319(5)	Cu13–S19	2.610(10)
Bi3–S10i	2.759(6)	Bi9–S24iv	3.003(6)	Bi17–S24	2.636(9)	Cu8–S5iv	2.319(5)	Cu14–S9	2.257(10)
Bi3–S19	2.776(8)	Bi9–S24iii	3.003(6)	Bi17–S35ii	2.739(6)	Cu8–S28xi	2.328(10)	Cu14–S11	2.341(11)
Bi3–S11	2.841(9)	Bi10–S16iv	2.738(6)	Bi17–S35i	2.739(6)	Cu8–S28x	2.405(10)	Cu14–S22iv	2.521(7)
Bi3–S33iv	2.862(7)	Bi10–S16iii	2.738(6)	Bi17–S25i	3.017(6)	Cu9A–Cu9B	0.745(12)	Cu14–S22iii	2.521(7)
Bi3–S33iii	2.862(7)	Bi10–S25	2.753(9)	Bi17–S25ii	3.017(6)	Cu9A–S13	2.301(7)	Cu14–Cu12ii	2.699(5)
Bi4–S3	2.597(9)	Bi10–S32	2.849(10)	Cu1–S27	2.304(10)	Cu9A–S13v	2.301(7)	Cu14–Cu12i	2.699(5)
Bi4–S23iv	2.637(6)	Bi10–S24iii	2.923(6)	Cu1–S6	2.342(10)	Cu9A–S17	2.309(14)	Fe1–S14xii	2.262(10)
Bi4–S23iii	2.637(6)	Bi10–S24iv	2.923(6)	Cu1–S29ii	2.365(6)	Cu9A–S23	2.47(2)	Fe1–S25ii	2.331(5)
Bi5–S5	2.612(8)	Bi11–S26	2.610(9)	Cu1–S29i	2.365(5)	Cu9B–S17	2.296(12)	Fe1–S25i	2.331(5)
Bi5–S7iv	2.679(6)	Bi11–S14	2.710(6)	Cu2–S21	2.317(10)	Cu9B–S13	2.377(7)	Fe1–S25ix	2.644(10)
Bi5–S7iii	2.679(6)	Bi11–S14viii	2.710(6)	Cu2–S31ii	2.341(6)	Cu9B–S13v	2.377(7)	Cu15xii–S14	2.262(10)
Bi5–S4ii	3.065(6)	Bi11–S31i	3.006(7)	Cu2–S31i	2.341(6)	Cu9B–S8	2.428(16)	Cu15iv–S25	2.331(5)
Bi5–S4i	3.065(6)	Bi11–S31ii	3.006(7)	Cu2–S21ix	2.412(10)	Cu10–S18	2.293(10)	Cu15ii–S25	2.331(5)
Bi5–Cu3	3.371(5)	Bi11–Cu2	3.361(5)	Cu3–S23	2.311(10)	Cu10–S32	2.360(11)	Cu15ix–S25	2.644(10)
Bi6–S27	2.700(9)	Bi12–S10	2.622(9)	Cu3–S4i	2.325(5)	Cu10–S22iii	2.418(6)		

Symmetry codes: (i) ½ + x, y – ½, z; (ii) ½ + x, ½ + y, z; (iii) x – ½, ½ + y, z; (iv) x – ½, y – ½ , z; (v) x, y – 1, z; (vi) ½– x, 3/2 – y, 1 – z; (vii) ½ – x, ½ – y, 1 – z; (viii) x, 1 + y, z; (ix) 1 – x, 1 – y,– z; (x) 1 – x, 1 – y, 1 – z; (xi) x – 1, y, z; (xii) 3/2 – x, ½ – y,– z; (xiii) 1 + x, y, z. Distances are expressed in Å.

do not form distorted octahedra, as one would expect in comparing kupčíkite and cuprobismutite.

The remaining Bi atoms, except Bi16, form pairs of BiS_{5+2} monocapped trigonal prims in the thin layers of the kupčíkite-like slabs: Bi5–Bi8, Bi6–Bi13, Bi7–Bi11. Polyhedron $Bi(16)S_{5+2}$ is an isolated monocapped trigonal prism in the composition zone $(001)_{pgr}$ (Fig. 7). The location of this coordination polyhedron fully corresponds to the tiling pattern of the cuprobismutite.

The Cu sites. In all structures of the cuprobismutite homologues, the tetrahedral coordination of copper is asymmetrical, transitional to trigonal–planar or, considering more distant ligands, trigonal–bipyramidal (Topa *et al*. 2003a). The same is true for pizgrischite (Fig. 7). In kupčíkite, Topa *et al*. (2003a) refined split Cu,Fe positions (not shown in the simplified Fig. 5). As discussed by Topa *et al*. (2003a) for kupčíkite, the splitting of the position is not automatically a consequence of Fe-for-Cu substitution. In pizgrischite, the Cu9 site is split and may contain some Fe. Refining the ratio Cu/Fe of all other sites resulted in full Cu occupancies for all sites except Cu15, which contains 23(10)% Fe.

All Cu atoms except Cu1 form pairs of CuS_4 tetrahedra *sensu lato*. Some of them are monotype (Cu2–Cu2, Cu4–Cu4, Cu8–Cu8, Cu10–Cu10), whereas the remaining pairs are not (Cu3–Cu9, Cu5–Cu7, Cu6–Cu14, Cu11–Cu12, Cu13–Cu15). The polyhedra containing Cu1 forms isolated $Cu(1)S_4$ tetrahedra in the composition zone (beige triangle in Fig. 7). The role of

$Cu(1)S_4$ as hinges between the $N = 5$ and 7 slabs has been discussed in a previous section. The coordination of four S atoms around Cu8 is distinctly tetrahedral, whereas Cu5 has three close ligands in a clear trigonal–planar arrangement [parallel to the (001) composition zone] and Cu9 has five ligands forming a distorted but fine trigonal bipyramid. All remaining CuS_4 tetrahedra show transitions in the sense described above.

The $Cu(13)S_4$ tetrahedron is attached to the $Bi(3)S_6$ octahedron (Fig. 7), as observed in cuprobismutite. The location of $Cu(15)S_4$, the counterpart of $Cu(13)S_4$ within the dark-grey-shaded composition zone (Fig. 7), is exactly where it has to be in the kupčíkite structure.

The Pb site. The isoelectronic Pb^{2+} and Bi^{3+} cannot be distinguished with the chosen experimental setup. Bond-valence estimates indicate substantial underbonding of "Bi18". Coordination polyhedra of bismuth in cuprobismutite homologues follow closely a hyperbolic correlation of opposing bonds, investigated originally by Trömel (1981) for Sb^{3+}, Te^{4+}, I^{5+} bonds with oxygen, and by Berlepsch *et al*. (2001) for bismuthinite derivatives (meneghinite homologues). Inspection of pairs of opposing Bi–S bonds of pizgrischite reveals that all except one fall on, or close to, the Bi–S hyperbola as defined by Berlepsch *et al*. (2001). Only "Bi18", with pairs of opposing Bi–S bonds of 2.996(7) Å and 3.026(7) Å, matches almost perfectly the intersection of the Pb–S hyperbola with the median line (x = y). Consequently, "Bi18" is regarded as the Pb site in pizgrischite, and accordingly has been labeled Pb1.

Chemical Structural Mineral Classification

According to the Chemical Structural Mineral Classification System of Strunz & Nickel (2001) and considering the chemical and structural features of the new PbS archetype sulfosalt, pizgrischite could be classified as a related mineral (pizgrischite subgroup) in the cuprobismutite series (2.JA.10).

Cu–Bi sulfosalts in Metamorphosed Pre-Alpine Deposits of Central Europe

In unmetamorphosed examples of polymetallic vein-type mineralization, emplectite is the most common Cu–Bi sulfosalt; wittichenite and cuprobismutite are less common. During metamorphism, however, a more complex paragenesis develops, and single phases such as emplectite or wittichenite rarely survive (Table 7). Complex Cu–Bi sulfosalts, such as pizgrischite, are characteristic of metamorphosed Cu–Bi vein-type deposits with a low content of Pb, which precludes the formation of minerals of the aikinite–bismuthinite series. These complex Cu–Bi sulfosalts can be very common at one locality, but rare elsewhere; this probably results partly from the difficulty in identifying these minerals, but also it reflects the fact that small variations in physical (cooling rate, P, T) and chemical variables [*e.g.*, $f(S_2)$ and Cu/Bi] can stabilize different phases. "Dry" and "wet" experiments in the system Cu–Bi–S made by Sugaki *et al*. (1981) and Wang (1994) show that complex sulfosalts like cuprobismutite, hodrushite and kupčíkite are not stable below ~300°C. For example, Sugaki *et al*. (1981) clearly demonstrated that below 316°C, cuprobismutite decomposes to emplectite and synthetic monoclinic $CuBi_3S_5$.

Acknowledgements

The manuscript greatly benefitted from an insightful review by Daniela Pinto and editorial care of Robert F. Martin. We are grateful to Stefan Ansermet and Stéphane Cuchet for their help during field work. We further thank Peter O. Baumgartner (SEM/EDS laboratory, Institute of Geology and Paleontology, UNIL, Lausanne) for help with the SEM. Special thanks to Gervais Chapuis (Laboratoire of Crystallography, EPFL, Lausanne) for single-crystal XRD facilities. Portions of this research were funded by the European Synchrotron Research Facility, Swiss–Norwegian Beam Line (project 01–01–30 to N. Meisser).

References

Baudin, T., Marquer, D., Barfety, J.-C., Kerchkove, C. & Persoz, F. (1995): A new stratigraphical interpretation of the Mesozoic cover of the Tambo and Suretta nappes: evidence for early thin-skinned tectonics (Swiss Central Alps). *C.R. Acad. Sci. Paris* **321**, 401-408.

Bérar, J.F. & Baldinozzi, G. (1998): XND code, from X-ray laboratory data to incommensurately modulated phases. Rietveld modelling of complex materials. *Int. Union of Crystallogr. – Commission of Powder. Diffr. Newsletter* **20**, 3-5.

Berlepsch, P., Makovicky, E. & Balić-Žunić, T. (2001): Crystal chemistry of meneghinite homologues and related sulfosalts. *Neues Jahrb. Mineral., Monatsh.*, 115-135.

Brugger, J. & Berlepsch, P. (1996): Description and crystal structure of fianelite $Mn_2V(V,As)O_7{\bullet}2H_2O$, a new mineral from Fianel, Val Ferrera, (Graubünden, Switzerland). *Am. Mineral.* **81**, 1270-1276.

Brugger, J., Berlepsch, P., Meisser, N. & Armbruster, T. (2003a): Ansermetite, $MnV_2O_6{\bullet}4H_2O$, a new mineral species with V^{5+} in five-fold coordination from Val Ferrera, eastern Swiss Alps. *Can. Mineral.* **41**, 1423-1431.

Brugger, J. & Gieré, R. (1999): As, Sb, and Ce enrichment in minerals from a metamorphosed Fe–Mn deposit (Val Ferrera, eastern Swiss Alps). *Can. Mineral.* **37**, 37-52.

Brugger, J. & Gieré, R. (2000): Origin and distribution of some trace elements in metamorphosed Fe–Mn deposits, Val Ferrera, eastern Swiss Alps. *Can. Mineral.* **38**, 1075-1101.

TABLE 7. OCCURRENCES WITH Bi–Cu–S SULFOSALTS IN CENTRAL EUROPE

Locality	Geochemical association	Sulfosalt-bearing mineral association	Metamorphic facies	References
Late Variscan Cu–Bi veins				
Faymont, Val d'Ajol, Vosges, France	Cu-Bi-Ba-F	Emp-Wtc-Td-Ccp-Brt-Fl-Qtz	None	Escande *et al.* (1973)
Brézouard, Vosges, France	Cu-Bi	Emp-Ccp-Bmt-Qtz	None	Weil *et al.* (1975)
Engelsbourg, Vosges, France	Cu-Bi-As-Zn-Pb	Ccp-Tn-Cos-Emp-Aik–Bmt-Bmt-Kob-Cbs-Qtz-Ank	None	Ruhlmann (1978)
Wittichen, Schwarzwald, Germany	Cu-Bi-Sb-Ba-Qtz	Wtc-Emp-Ccp-Td-Brt	None	Walenta (1992)
Tannenbaum, Saxony, Germany	Cu-Bi	Emp-Ccp-Gn-Cal-Dol-Sd-Fl-Qtz	None	Haake *et al.* (1994)
Krupka, Bohemia, Czech Republic	Cu-Bi-As-Sn-Mo-W	Aik–Bmt-Ccp-Bmt-Cbs-Emp-Gn-Apy-Mlb-Cst-Qtz-Scl	None	Paulis & Haake (1995)
Banská Hodruša, Carpathians, Slovakia	Cu-Bi-Fe	Ccp-Hod-Wtc?-Hem-Qtz	None	Koděra *et al.* (1970)
Piz Grisch, Graubünden, Switzerland	Cu-Bi-Fe-Zn-Sb	Pgr-Emp-Aik–Bmt-Ccp-Td-Sp-Qtz	Greenschist	This study
Variscan greenstone-belt W deposit				
Felbertal, Salzburg, Austria	Cu-Bi-Pb-Fe-Zn	Kpk-Mak-Hod-Cbs-Aik–Bmt-Ccp-Po-Mlb-Sp-Bi-Qtz	Greenschist to low amphibolite	Topa *et al.* (2003b)
Pre-variscan (?) stratabound Cu–Bi deposits				
Baicolliou, Grimentz, Wallis, Switzerland	Cu-Bi-As-Co-Sn	Cbm-Em-Wtc-Ccp-Tn-Cbt-Cst-Ank-Qtz	Greenschist	Picot & Johan (1977), Ansermet & Meisser (in prep.)
Spicherli, Turtmann, Wallis, Switzerland	Cu-Bi	Kpk-Ccp-Ank-Qtz	Greenschist	Ansermet & Meisser (in prep.)
Variscan or alpine Ni-Co-Bi-Cu-As veins				
Kaltenberg, Turtmann, Wallis, Switzerland	Cu-Bi-Pb	Ho-Bi-Dol	Greenschist	Ansermet & Meisser (in prep.)
Čierna Lehota, Carpathians, Slovakia	Cu-Bi-Ag-As-Zn-Pb	Kpk-Cbs-Hod-Bi-Mat-Tn-Ccp-Sp-Gn-Qtz	Zeolite	Pršek *et al.* (2005)

Notes: Aik–Bmt: aikinite–bismuthinite series of minerals, Ank: ankerite, Apy: arsenopyrite, Bi: native bismuth, Bmt: bismuthinite, Brt: barite, Cal: calcite, Cbs: cuprobismutite, Cbt: cobaltite, Ccp: chalcopyrite, Cos: cosalite, Cst: cassiterite, Dol: dolomite, Emp: emplectite, Fl: fluorite, Gn: galena, Hem: hematite, Hod: hodrushite, Kob: kobellite, Kpk: kupčíkite, Mak: makovickyite, Mat: matildite, Mlb: molybdenite, Po: pyrrhotite, Pgr: pizgrischite, Qtz: quartz, Scl: scheelite, Sd: siderite, Sp: sphalerite, Td: tetrahedrite, Tn: tennantite, Wtc: wittichenite.

BRUGGER, J., KRIVOVICHEV, S., KOLITSCH, U., MEISSER, N., ANDRUT, M., ANSERMET, S. & BURNS, P.C. (2003b): Description and crystal structure of manganlotharmeyerite, $Ca(Mn^{3+},Mg)_2\{AsO_4[AsO_2(OH)_2]\}_2(OH,H_2O)_2$, from the Starlera Mn deposit, Swiss Alps, and a redefinition of lotharmeyerite. *Can. Mineral.* **40**, 1597-1608.

BURNS, P.C. (1998): CCD area detectors of X-rays applied to the analysis of mineral structures. *Can. Mineral.* **36**, 847-853.

DIETRICH, V., HUONDER, N. & RYBACH, L. (1967): Uranvererzung im Druckstollen Ferrera – Val Niemet. *Beitr. Geologie der Schweiz, Geotech. Ser.* **44**.

ESCANDE, J.C., JOHAN, J., LOUGNON, J., PICOT, P. & PILLARD, F. (1973): Note sur la présence de minéraux de bismuth dans un filon de barytine et fluorine à Faymont, près Le Val-d'Ajol (Vosges). *Bull. Soc. fr. Minéral. Cristallogr.* **96**, 398-399.

ESCHER, E. (1935): Erzlagerstätten und Bergbau im Schams, in Mittelbünden und in Engadin. *Beitr. Geologie der Schweiz, Geotech. Ser.* **18**.

EUROPEAN SYNCHROTRON RADIATION FACILITY (2005): *A Light for Science*. ESRF, Grenoble, France.

GRÜNENFELDER, M. (1956): Petrographie des Roffnakristallins in Mittelbünden und seine Eisenvererzungen. *Beitr. Geologie der Schweiz, Geotech. Ser.* **18**.

HAAKE, R., FLACH, S. & BODE, R. (1994): *Mineralien und Fundstellen Deutschland* **2**. Bode Verlag GmbH, Haltern, Germany.

KODĚRA, M, KUPČÍK, V. & MAKOVICKY, E. (1970): Hodrushite; a new sulphosalt. *Mineral. Mag.* **37**, 641-648.

MAKOVICKY, E. (1989): Modular classification of sulphosalts: current status, definition and application of homologous series. *Neues Jahrb. Mineral., Abh.* **160**, 269-297.

MARQUER, D., CHALLANDES, N. & BAUDIN, T. (1996): Shear zone patterns and strain distribution at the scale of a Penninic nappe: the Suretta nappe (eastern Swiss Alps). *J. Struct. Geol.* **18**, 753-764.

MARQUER, D., CHALLANDES, N. & SCHALTEGGER, U. (1998): Early Permian magmatism in Briançonnais terranes; Truzzo Granite and Roffna rhyolite (eastern Penninic nappes, Swiss and Italian Alps). *Schweiz. Mineral. Petrogr. Mitt.* **78**, 397-414.

MEISSER, N., ANSERMET, S., BRUGGER, J. & WÜLSER, P.A. (2004) : Alpine metamorphised ore deposits: gardens of rare or new minerals for mineralogical museums. Mineralogy & Museum 5th Congress (Paris). *Bull. liaison Soc. fr. Minéral. Cristallogr.* **16**, 58.

PAULIS, P. & HAAKE, R. (1995): Zur Geologie und Mineralogie der Lagerstätten in der Umgebung von Krupka (Graupen) bei Teplice (Teplitz) in Böhmen. *Mineralien Welt* **6**, 46-56.

PICOT, P. & JOHAN, Z. (1977): *Atlas des Minéraux Métalliques*. BRGM, Orléans, France (Mém. **90**).

PRŠEK, J., MIKUŠ, T., MAKOVICKY, E. & CHOVAN, M. (2005): Cuprobismutite, kupčíkite, hodrushite and associated sulfosalts from the black shale hosted Ni–Bi–As mineralization at Čierna Lehota, Slovakia. *Eur. J. Mineral.* **17**, 155-162.

RUHLMANN, F. (1978): Une paragenèse bismuthifère dans les filons de la mine d'Engelsbourg (Sainte-Marie-aux-Mines, Vosges). *Bull. Soc. fr. Minéral. Cristallogr.* **101**, 570-572.

SHELDRICK, G.M. (1997): *SHELXL–97 and SHELXS–97. Programs for Crystal Structure Determination*. University of Göttingen, Göttingen, Germany.

SOMMERAUER, J. (1972): Radiometrische und erzpetrographische Untersuchungen im Muskovit–Alkalifeldspat-Augengneis von Alp Taspegn, Kanton Graubünden. *Beitr. Geologie der Schweiz, Geotech. Ser.* **48**.

STRUNZ, H. & NICKEL, E.H. (2001): *Strunz Mineralogical Tables. Chemical Structural Mineral Classification System* (9th ed.). E. Schweitzerbart'sche Verlagbuchhandlung (Nägele u. Obermiller), Stuttgart, Germany.

SUGAKI, A., KITAKAZE, A. & HAYASHI, K. (1981): Synthesis of minerals in the Cu–Fe–Bi–S system under hydrothermal condition and their phase relations. *Bull. Soc. fr. Minéral. Cristallogr.* **104**, 484-495.

TOPA, D., MAKOVICKY, E. & BALIĆ-ŽUNIĆ, T. (2003b): Crystal structures and crystal chemistry of members of the cuprobismutite homologous series of sulfosalts. *Can. Mineral.* **41**, 1481-1501.

TOPA, D., MAKOVICKY, E., BALIĆ-ŽUNIĆ, T. & PAAR, W. (2003a): Kupčíkite, $Cu_{3.4}Fe_{0.6}Bi_5S_{10}$, a new Cu–Bi sulfosalt from Felbertal, Austria, and its crystal structure. *Can. Mineral.* **41**, 1155-1166.

TRÖMEL, M. (1981): Abstandskorrelationen bei der Tellur(IV)-Sauerstoff- und Antimon(III)-Sauerstoff-Koordination. *Z. Kristallogr.* **154**, 338–339.

WALENTA, K. (1992): *Die Mineralien des Schwarzwaldes und ihre Fundstellen*. Weise Verlag, Munich, Germany.

WANG, N. (1994): The Cu–Bi–S system: results from low-temperature experiments. *Mineral. Mag.* **58**, 201-204.

WEIL, R., SIAT, A. & FLUCK, P. (1975): Espèces minérales inédites ou rares des Vosges. *Sci. Géol. Bull.* **28**, 261-282.

Received May 26, 2006, revised manuscript accepted March 8, 2007.